Eur. Phys. J. A **11**, 121–124 (2001)

THE EUROPEAN
PHYSICAL JOURNAL A

Short Note

Investigation of the magnetic rotation in ^{196}Pb

G. Kemper[1], A. Dewald[1], I. Wiedenhöver[1], R. Peusquens[1,a], S. Kasemann[1], K.O. Zell[1], P. von Brentano[1], H. Hübel[2], S. Chmel[2], A. Görgen[2], D. Bazzacco[3], R. Venturelli[3], S. Lunardi[3], D.R. Napoli[4], F. Hannachi[5], A. Lopez-Martens[5], R. Krücken[6], J.R. Cooper[6], R.M. Clark[7], M.A. Deleplanque[7], I.Y. Lee[7], A.O. Machiavelli[7], and F.S. Stephens[7]

[1] Institut für Kernphysik, Universität zu Köln, Zülpicher Str. 77, D-50937 Köln, Germany
[2] Institut für Strahlen- und Kernphysik, Universität Bonn, Bonn, Germany
[3] Dipartimento di Fisica, Università and INFN Sezione Padova, Italy
[4] INFN, Laboratori Nazionali di Legnaro, Italy
[5] Institut de Physique Nucleaire, 91405 Orsay, Cedex, France
[6] A.W. Wright Nuclear Structure Laboratory Yale University, New Haven, CT 06520, USA
[7] Lawrence Berkeley National Laboratory, Berkeley, CA 94720, USA

Received: 3 May 2001
Communicated by D. Schwalm

Abstract. Lifetimes for low-lying members of the irregular $\Delta I = 1$ band in ^{196}Pb have been measured by means of the EUROBALL spectrometer using the coincidence recoil distance technique. The ^{164}Dy(^{36}S,4n)^{196}Pb reaction at a beam energy of 168 MeV was used. The data were analyzed with the differential decay-curve method (DDCM). A characteristic drop in the reduced transition probabilities with increasing angular momentum was observed in agreement with predictions by the semiclassical model for the shears mechanism.

PACS. 21.10.Ky Electromagnetic moments – 21.10.Re Collective levels – 23.20.-g Electromagnetic transitions – 27.80.+w $190 \leq A \leq 219$

In recent years cascades of enhanced magnetic dipole ($M1$) transitions have been observed in the neutron-deficient Pb nuclei (see refs. [1,2] for recent reviews). A number of similar bands were found in the $A \sim 110$ and $A \sim 140$ regions. The properties of these bands have been successfully described by the the tilted axis cranking (TAC) model by Frauendorf [3] as well as the semiclassical model by Macchiavelli *et al.* [4–6]. In these models the band-head configuration in the Pb isotopes arises from the perpendicular coupling of the angular momenta of high-K protons and high-j neutron-holes. This interpretation has been supported by the results of a recent g-factor measurement [7]. Angular momentum in the bands is gained by a simultaneous step-by-step re-orientation of the proton-particle and the neutron-hole angular momenta into the direction of the total angular momentum. One can picture this as the closing of the blades of a pair of shears, leading to the name “shears bands” [8].

The characteristic prediction of this shears mechanism is that within the bands the reduced matrix element $B(M1)$ for the dipole transitions decrease with increasing angular momentum, since the $B(M1)$ values are proportional to the components of the magnetic moments perpendicular to the total angular momentum. Recent lifetime measurements in the light Pb isotopes [9–11] have experimentally confirmed this behavior of the $B(M1)$ values.

In ^{196}Pb four rather regular bands of $M1$ transitions have been observed. For band 2 [12] the linking transitions to the yrast levels are known, allowing the determination of the spins and the excitation energies of states within this band. As most of the intensity from the decay out of this band proceeds through the 11^- state [13], a two proton excitation $\pi(s_{1/2}^{-2}h_{9/2}i_{13/2})$ coupled to two neutron holes was assigned to this band [12–14].

The most strongly populated band (band 1) in this nucleus has been previously reported as an irregular sequence of transitions [13]. With a change in the ordering of some transitions, according to their intensities, band 1 can be viewed as a regular band with a band crossing [12]. Due to the comparison to the neigboring even-even isotope ^{198}Pb, it has been suggested that the configurations $AE11$ or $AF11$ apply below the band crossing and $ABCE11$ or

[a] e-mail: rp@ikp.uni-koeln.de

$ABCF11$ apply above the band crossing [15] following the nomenclature in ref. [8]. $B(M1)$ values for high-lying transitions above the band crossing were determined from a measurement using the Doppler-shift attenuation method (DSAM) [10]. Spins and parities of the states in this band have recently been reported by Singh *et al.* [16].

In this short note we report on a lifetime experiment for ^{196}Pb employing the recoil distance method (RDM) from which lifetimes for states near the band head of band 1 in ^{196}Pb have been extracted.

The RDM experiment for ^{196}Pb was performed at the XTU TANDEM accelerator of the INFN in Legnaro, Italy. The ^{164}Dy(^{36}S,4n)^{196}Pb reaction at a beam energy of 168 MeV was used to populate excited states in ^{196}Pb. The target consisted of a 0.9 mg/cm^2 ^{164}Dy evaporated onto a 1.4 mg/cm^2 tantalum foil. The recoiling ^{196}Pb nuclei were stopped in a 12 mg/cm^2 gold foil. Target and stopper foil were mounted inside the Cologne coincidence plunger apparatus.

Gamma rays from ^{196}Pb were detected by the EUROBALL spectrometer. The plunger apparatus, which is especially designed for $\gamma\gamma$-coincidence measurements, was installed in the EUROBALL spectrometer for the first time. An average of 3.4 billion coincidence events with an unsuppressed fold of at least five recorded on magnetic tape at 15 target-to-stopper distances in the range from 1 μm to 382 μm with respect to the electrical contact of the foils in runs of about 8-10 hours each. The EUROBALL detectors can be grouped in six rings, with all detectors of a given ring showing approximately the same angle with respect to the beam axis. Five of the rings can be used for a lifetime analysis since they provide a sufficient Doppler shift to separate shifted and unshifted components for the transitions of interest. The actual angles of the detectors in the rings were 149°-163°, 130°-138°, 80°-107°, 52.2°, 34.6° and 15.5°. The data was unfolded and sorted into separate $\gamma\gamma$-matrices for each distance and detector ring combination.

The rather poor peak-to-total ratio of the spectra, in particular for the Cluster detectors, was most probably caused by very high thresholds cutting the energy signal already at 200-300 keV in the coincidence mode thus preventing an efficient addback of compton scattered events. Nevertheless, the established $\Delta I = 1$ bands in ^{196}Pb were observed. The states in the shears bands exhibit rather short intrinsic lifetimes. However, due to the relatively long feeding times, on the order of about 2 ps, it was possible to extract lifetimes of the three lowest excited states in band 1 of ^{196}Pb.

The lifetimes of the levels of interest were determined with the differential decay curve method (DDCM) [17]. As shown in refs. [17,18] lifetimes can be calculated from RDM coincidence data for each target-to-stopper distance x by the relation:

$$\tau = \frac{I_{\rm su}^{CA}(x) - \alpha I_{\rm su}^{CB}(x)}{v \cdot \frac{\rm d}{{\rm d}x} I_{\rm ss}^{CA}(x)}\,, \qquad (1)$$

Table 1. Lifetime results for band 1 in ^{196}Pb. The level lifetimes along with the energies of the de-exciting γ-rays are given. The reduced transition probabilities $B(M1)$ are presented (W.u. stands for Weisskopf unit), under the assumption that the transitions are of pure $M1$ character.

I^π ($\hbar$)	E_γ (keV)	τ (ps)	$B(M1)$ (μ_N^2)	$B(M1)$ (W.u.)
18^+	193	1.28 (22)	2.4 $(^{+0.5}_{-0.3})$	1.3 $(^{+0.3}_{-0.2})$
19^+	315	0.96 (20)	1.4 $(^{+0.4}_{-0.2})$	0.8 $(^{+0.2}_{-0.1})$
20^+	375	1.34 (50)	0.7 $(^{+0.4}_{-0.2})$	0.4 $(^{+0.2}_{-0.1})$

where

$$\alpha = \frac{I^{CA}}{I^{CB}} = \frac{I_{\rm su}^{CA} + I_{\rm ss}^{CA}}{I_{\rm su}^{CB} + I_{\rm ss}^{CB}}\,.$$

Here v is the recoil velocity measured to $v/c = 1.79(5)\%$. The level of interest is populated by transition B and depopulated by transition A. The intensities $I_{\rm su,ss}^{CA,B}$ are the number of events for which the unshifted (u) and shifted (s) component of the transitions A and B is coincident with the shifted component of an indirect feeding transition C. The derivative $\frac{\rm d}{{\rm d}x} I_{\rm ss}^{CA}(x)$ can be determined by the usual ratio of differences. It is obvious that the obtained values for τ are most reliable in the region of the largest slope.

Gated spectra with gates on shifted components of the feeding transitions of the band were produced for each distance and each detector ring. Due to the insufficient statistics the spectra taken at average polar angles of 156°, 134°, 52° and 34° were modified in a way that the Doppler-shifted peaks came to the same position as those in the spectra taken at 15°, while the position of the stopped peaks remained unchanged. With this technique it was possible to sum up the complete statistics for each distance in one single spectrum which was then analyzed to determine the intensities of the transitions of interest. Figure 1 shows such spectra at three different target-to-stopper distances.

The measured lifetimes of the three low-lying levels in the investigated band are given in table 1 in addition to the corresponding $B(M1)$ values determined under the assumption that the transitions are of pure M1 character. Spins and parities for the levels of band 1 in ^{196}Pb are taken from ref. [16].

Figure 2 shows the $B(M1)$ values determined in this work together with those from ref. [10] plotted as a function of the angular momentum $I(\hbar)$. As mentioned earlier, band 1 undergoes a crossing at angular momentum values around 21–23$\hbar$. One clearly observes the expected decreasing behavior with increasing spin below and above the band crossing, respectively. Below the band crossing the $B(M1)$ values fall from 2.4 to 0.7 μ_N^2. Above the band crossing, at the 25 $\hbar$ level, the $B(M1)$ values jump to $\approx 9\mu_N^2$ and then decrease down to 2 μ_N^2 with increasing spin.

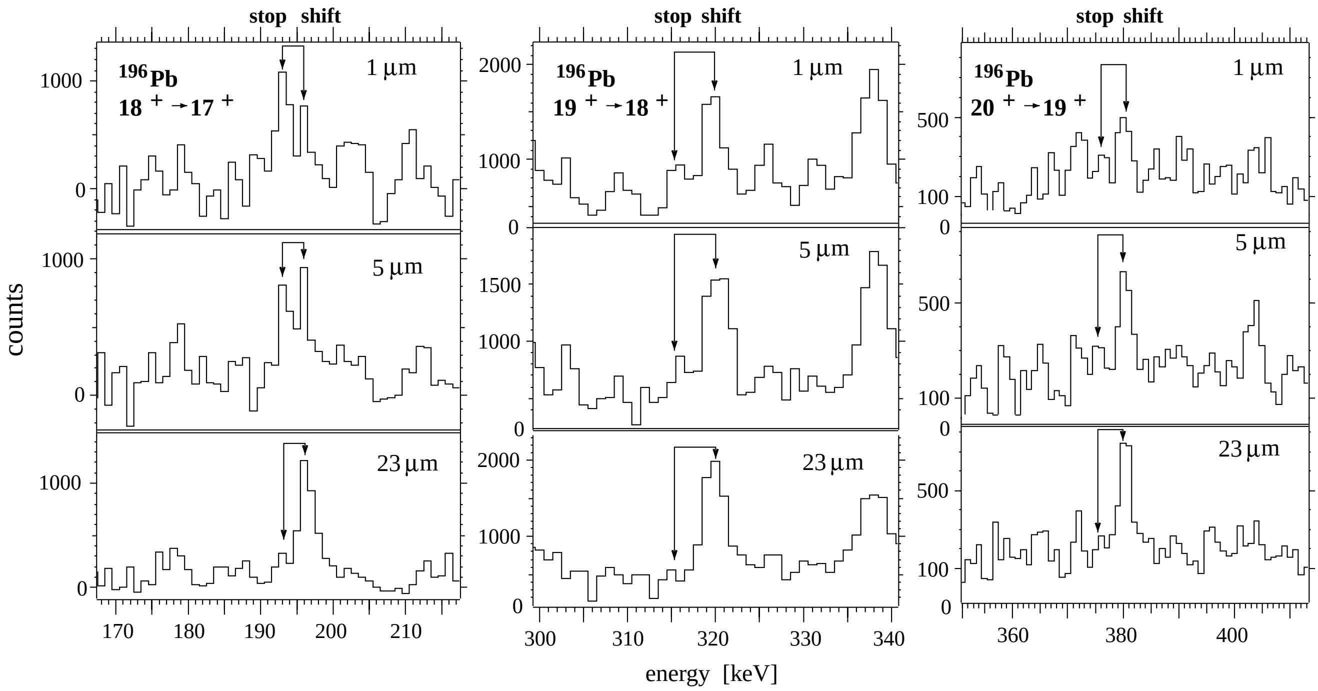

Fig. 1. $\gamma\gamma$-coincidence spectra taken at different target-to-stopper distances showing both shifted and unshifted peaks of the 193 keV (left), 315 keV (middle) and 375 keV transitions (right) of the investigated $\Delta I = 1$ band. Gates were placed on the shifted components of feeding transitions. The spectra result from summed up gated spectra taken at five different polar angles. The Doppler-shifted energies are corrected to correspond to a polar angle of 15.5°. (See text for detailed explanation.)

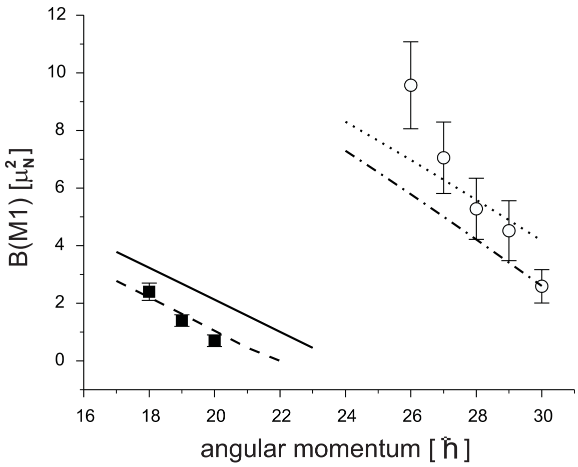

Fig. 2. Experimental $B(M1)$ values for band 1 in ^{196}Pb from the present RDM experiment (squares) and a previous DSAM experiment [10] (circles). The lines represent the results of calculations using the semiclassical model by Macchiavelli *et al.* for the suggested configurations $AE11$ (solid line) and $AF11$ (dashed line) below the band crossing and ABCE11 (dotted line) and ABCF11 (dash-dotted line) above the bandcrossing.

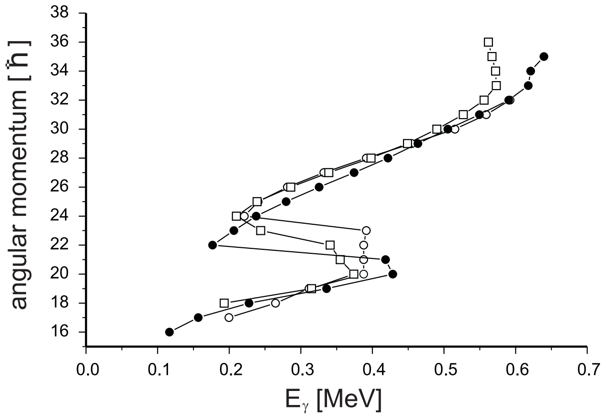

Fig. 3. Spin as a function of γ-ray energy E_γ (rotational frequency) for band 1 in ^{196}Pb, band 1 and band 5 in ^{198}Pb. Data are taken from refs. [15,16].

The energy spectrum of band 1 in ^{196}Pb is very similar to those of band 1 and band 5 in ^{198}Pb [15] (see fig. 3). On the basis of TAC calculations, the configuration $AE11$, $\pi(s_{1/2}^{-2}h_{9/2}i_{13/2})11^- \otimes \nu(i_{13/2}f_{5/2})$, is assigned to band 1 of ^{198}Pb below the band crossing and ABCE11 above the crossing where two additional $\nu i_{13/2}$ (BC) quasiparticles are aligned [15]. For band 5, the configuration $AF11/ABCF11$ was attributed [15]. Therefore it is expected that also for ^{196}Pb one of these configurations can be assigned to band 1.

Alternatively, we used the semiclassical approach by Macchiavelli *et al.* [4–6] to gain a simple understanding of the magnitude and spin dependence of the $B(M1)$ values. The shears angle θ as well as the corresponding $B(M1)$ value are calculated from the spin vectors j_π and j_ν for every state of the band. Also the energy spectrum is calculated assuming an effective interaction between the quasi-protons and quasi-neutrons of the type

$$V_{\pi\nu}(\theta) = V_0 + V_2 P_2(\cos\theta)\,.$$

In fig. 2 the experimental $B(M1)$ values are compared to calculated values based on this semiclassical description for the configurations $AF11/ABCF11$ ($j_\nu = 8/18\hbar$) and $AE11/ABCE11$ ($j_\nu = 9/19\hbar$). An effective gyromagnetic factor of $g_{\rm eff} = g_\pi - g_\nu = 0.9$ was used in these calculations. The agreement of experimental and calculated values is rather good especially for the $AF11/ABCF11$ ($j_\nu = 8/18\hbar$) configuration although the $AE11/ABCE11$ ($j_\nu = 9/19\hbar$) configuration cannot be completely ruled out.

In summary, we have measured lifetimes of states near the band head in shears band 1 in ^{196}Pb. The resulting $B(M1)$ values show the characteristic drop with increasing angular momentum characteristic for the shears mechanism. The $B(M1)$ values below and above the band crossing in this shears band can be quantitatively reproduced in the the framework of the semiclassical model for the shears bands [4–6]. The TAC configurations $AF11$ and $ABCF11$ above and below the crossing, respectively, are most compatible with the experimental data. However, on the basis of the $B(M1)$ values alone the configurations $AE11$ and ABCE11 cannot be completely ruled out.

This work was supported in part by BMBF, the U.S. Department of Energy and the European Union TMR Programme under grant Nos. DE-FG02-91ER-40609, contract No. DE-AC03-765F-00098 and contract No. ERBFMGECT980110.

References

1. R.M. Clark, A.O. Macchiavelli, Annu. Rev. Nucl. Part. Sci. **50**, 1 (2000).
2. S. Frauendorf, Rev. Mod. Phys. **73**, 463-516 (2001).
3. S. Frauendorf, Nucl. Phys. A **557**, 259c (1993).
4. A.O. Macchiavelli *et al.*, Phys. Rev. C **57**, R1073 (1998).
5. A.O. Macchiavelli *et al.*, Phys. Rev. C **58**, R621 (1998).
6. A.O. Macchiavelli *et al.*, Phys. Lett. B **450**, 1 (1999).
7. S. Chmel *et al.*, Phys. Rev. Lett. **79**, 2002 (1997).
8. G. Baldsiefen *et al.*, Nucl. Phys. A **574**, 521 (1994).
9. R.M. Clark *et al.*, Phys. Rev. Lett. **78**, 1868 (1997).
10. R.M. Clark *et al.*, Phys. Lett. B **440**, 251 (1998).
11. R. Krücken *et al.*, Phys. Rev. C **58**, R1876 (1998).
12. G. Baldsiefen *et al.*, Z. Phys. A **355**, 337 (1996).
13. J.R. Hughes *et al.*, Phys. Rev. C **47**, R1337 (1993).
14. R.M. Clark *et al.*, Nucl. Phys. A **562**, 121 (1993).
15. A. Görgen *et al.*, Nucl. Phys. A **683**, 108 (2001).
16. A.K. Singh *et. al.*, Verh. DPG, Hadr. und Kerne, Erlangen 2001, p. 37, unpublished.
17. A. Dewald, S. Marissopulos, P. von Brentano, Z. Phys. A **334**, 163 (1989).
18. G. Böhm, A. Dewald, P. Petkov, P. von Brentano, Nucl. Instrum. Methods A **329**, 248 (1993).